Chinese Chemical Letters 33 (2022) 2473–2476

Contents lists available at ScienceDirect

Chinese Chemical Letters

journal homepage: www.elsevier.com/locate/cclet

1,1′-Binaphthol annulated perylene diimides: Aggregation-induced emission enhancement and chirality inversion

Yang Zhang[a], Juejun Wang[a], Hongming Chen[b], Meijin Lin[a,b,*]

[a] Key Laboratory of Molecule Synthesis and Function Discovery, College of Chemistry, Fuzhou University, Fuzhou 350116, China
[b] College of Materials Science and Engineering, Fuzhou University, Fuzhou 350116, China

ARTICLE INFO

Article history:
Received 29 July 2021
Revised 22 November 2021
Accepted 23 November 2021
Available online 27 November 2021

Keywords:
Perylene diimides
1,1′-Binaphthol
Aggregation-induced emission enhancement
Chirality inversion

ABSTRACT

Aggregation-induced emission enhancement and aggregation-induced chirality inversion are two individual phenomena for the enantiomerically pure organic dyes in the aggregates. Herein we reported for the first time that these two interesting phenomena could be observed simultaneously in the aggregated states of enantiomerically pure *S*/*R*-1,1′-binaphthol annulated perylene diimides, in which two perylene diimides moieties were bridged by *S*/*R*-1,1′-binaphthol (BINOL) at the bay positions. Owing to the rotatable C2 axes between two naphthol annulated perylene diimides moieties, both of them display intrinsic behaviors of aggregation-induced emission enhancements. At the same time, due to the steric hindrances in the imide and methoxy positions, the neighboring two π-systems of these two unique polycyclic aromatic imides in poor solvents are preferable to adopt a cross-stacking mode and thus form helical X-aggregates of opposite chirality (M/P) with chirality inversion characteristics in their circular dichroism and circularly polarized luminescence spectroscopic studies.

Organic conjugated luminescent materials have attracted great attention in the past years owing to their excellent optical-electronic properties and wide applications [1,2]. Nevertheless, these studies have always been plagued by the aggregation-caused quenching (ACQ) behaviors due to the formation of excimers or exciplexes *via* π-π stacking interactions in the solid or aggregated states [3]. To overcome these adverse behaviors, two close phenomena, aggregation-induced emission (AIE) [4] and aggregation-induced emission enhancement (AIEE) [5], have been reported by Tang *et al.* in 2001. Subsequently, tremendous AIE or AIEE molecules with rotatable C–C bonding structures have been synthesized [6–11]. On the other hand, chirality inversion is an intriguing phenomenon for chiral materials [12,13]. In general, it is rather difficult to achieve chirality inversion for optically pure organic compounds within the molecules [14,15] but possible in the aggregated states [16]. Considering both emission enhancement and chirality inversion occur in the aggregates, the simultaneous observation of AIEE and aggregation-induced chirality inversion phenomena can be anticipated for chiral π-conjugated systems with rotatable C–C bonding structures. Herein, we reported that this concept is indeed viable.

For the realization of this concept, we have synthesized a pair of enantiomerically pure *R*/*S*-1,1′-binaphthol annulated perylene diimides, **R-BPDH** and **S-BPDH** (Fig. 1). Wherein, perylene diimides (**PDIs**) act as luminescent chromophore entities as their outstanding optical, electronic and light fastness properties [17–20], while 1,1′-binaphthol (BINOL) moieties play as the chiral units with the rotatable C–C bonding structures. Indeed, the BINOL derivatives have also been demonstrated to be an attractive class of organic dyes with remarkable AIEE and circularly polarized luminescence (CPL) properties [21–23]. In addition, the incorporation of **PDIs** entities into BINOL units at the 5,6-positions to form helical π-clips with large dihedral angles, together with the introduction of steric substituents at the imide positions, which will help to adopt a cross-stacking mode [24] and thus form helical X-aggregates of opposite chirality (M/P). As expected, the AIEE phenomena are indeed observed in the fluorescent spectra of both two unique polycyclic aromatic imides in a mixture solvent of dichloromethane (DCM)/methylcyclohexane (MCH), while the circular dichroism (CD) and CPL spectroscopic studies show chirality inversion characteristics.

As the known at bay area aryl-substituted **PDIs** that were usually prepared by transition metal catalysis [25], the present **R-BPDH** and **S-BPDH** are synthesized in a yield of 79% and 82%, respectively (Scheme 1). They were obtained by the combination of mono-brominated **PDIs** [26] and *R*/*S*-1,1′-binaphthol [27] through a

* Corresponding author.
E-mail address: meijin_lin@fzu.edu.cn (M. Lin).

https://doi.org/10.1016/j.cclet.2021.11.069
1001-8417/

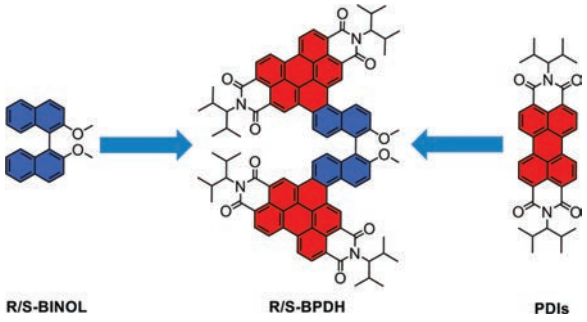

Fig. 1. Chemical structures of **R/S-BINOL**, **R/S-BPDH** and **PDIs**.

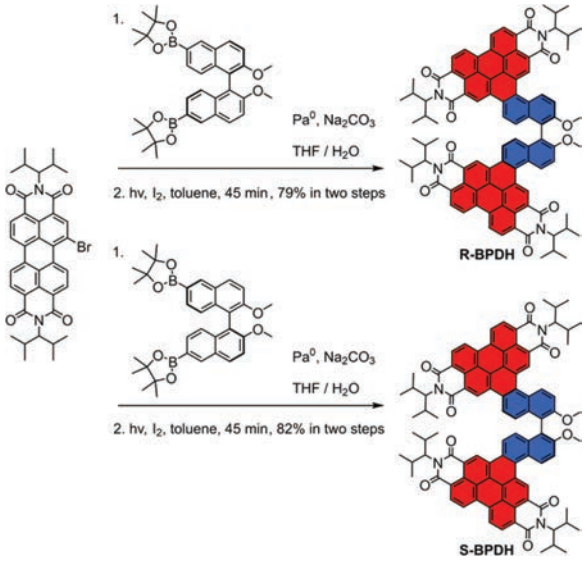

Scheme 1. Synthesis of enantiomerically pure **R/S-BPDH.**

palladium-catalyzed Suzuki cross-coupling reaction followed by a photocyclization in the presence of catalytic amount I_2 in toluene solutions upon the irradiation of a mercury lamp for 45 min. The chemical structures of **R/S-BPDH** have been assigned by 1- and 2-D NMR spectroscopy (Figs. S1-S12 in Supporting information) as well as by high-resolution mass spectral analyses (Figs. S13-S17 in Supporting information), which unequivocally confirm their conjugated structures with *R*/*S*-1,1′-binaphthol annulated at the bay positions of perylene diimides.

The steady-state optical properties of **R/S-BPDH** in DCM have been explored by UV–vis absorption and fluorescence spectroscopy (Fig. 2 and Fig. S21 in Supporting information). At room temperature, the UV–vis spectra of **R/S-BPDH** show very close absorption maxima at 505 nm, which are shifted hypsochromically by *ca.* 827 cm^{-1} in comparison to that of the parent PDI without bay substituents (absorption maximum at *ca.* 527 nm [28]). And it is consistent with the spectral shift of bay-extended **PDIs** [29]. Besides, due to the π-extension at the bay position, the maximum molar extinction coefficients of 124,397 $L\,mol^{-1}\,cm^{-1}$ in the **R/S-BPDH** are almost twice to **PDIs** for 69,298 $L\,mol^{-1}\,cm^{-1}$. The most remarkable feature of the absorption spectra is, however, the partial loss of vibronic fine structure for both **R/S-BPDH**. The UV–vis spectra in different polarity solvents show remarkable solvatochromism with different absorption maxima and spectral shapes (Figs. S19 and S20, Tables S1 and S2 in Supporting information). Especially in the polar solvent methanol, almost no vibronic fine structure could be observed. Accordingly, the absorption properties are mainly related to two factors: (1) a significant intramolecular charge transfer (ICT) from the electron-donating methoxyl substituents of BINOL units to the electron-deficient PDI core (the dominant factor); (2) the helical distortion of the aromatic system evoked by sterical congestion bridged with BINOL units in the bay area (the cooperative factor).

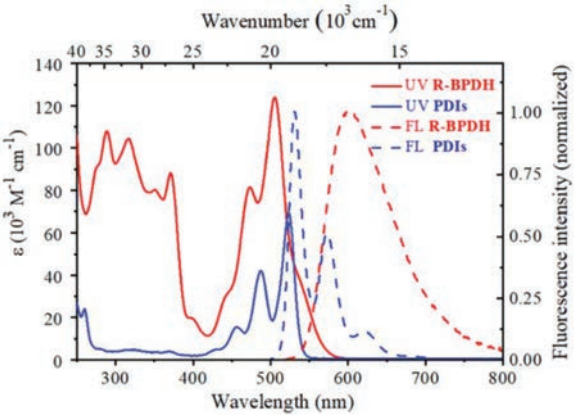

Fig. 2. UV–vis absorption (solid line) and normalized emission fluorescence (FL) spectra (dotted line, $\lambda_{ex} = 470$ nm, 5×10^{-6} mol/L) of **R-BPDH** and referenced **PDIs** in DCM.

Similar conclusions can be drawn from the fluorescence spectra of **R/S-BPDH** that exhibit relatively broad emission bands with large Stokes shifts at 601 nm, and fluorescence quantum yields of 72% and 73%, respectively. The fluorescence quantum yields of **R/S-BPDH** in solid state are recorded too (Tables S1 and S2). And it could be further corroborated by their electrochemical and theoretical studies. As shown in Fig. S18 (Supporting information), the cyclic voltammetry (CV) curves of **R/S-BPDH** in DCM exhibit close features with two reduction potentials at −1.07 and −1.27 V *vs.* Fc/Fc^+, which are slightly decreasing compared to those of bay-unsubstituted **PDIs** (−0.95 and −1.17 V *vs.* Fc/Fc^+, respectively). Thus, the fusion of BINOL into **PDIs** at the bay positions results in decreasing reduction potentials and increasing LUMO energy levels, thus enlarging the HOMO and LUMO energy gaps. This result can be proved by the density functional theoretical calculations (DFT). Compared with the bay-unsubstituted **PDIs** [30], the **R/S-BPDH** presented a higher energy of HOMO orbits from −6.09 eV to −5.83 eV, while those of LUMO orbits from −3.60 eV to −3.19 eV. As a result, the E_{gap} ($E_{gap} = E_{LUMO} - E_{HOMO}$) of **R/S-BPDH** are increasing to 2.64 eV in comparison to that of bay-unsubstituted **PDIs** (2.49 eV). Furthermore, the electrons in LUMO orbits of **R/S-BPDH** are mainly distributed in electron-deficient PDI cores (Fig. 3), while those in the HOMO orbits are delocalized over the electron-donating BINOL scaffolds and partly over perylene units. From these separated molecular orbits, a significant ICT is anticipated upon irradiations, which helps for the understanding of their solvatochromism.

The enantiomerically pure structural characteristics of **R/S-BPDH** have been investigated by the CD and CPL spectroscopy in DCM. As shown in Fig. 4, a pair of clear mirror-image CD spectra could be observed for **R/S-BPDH**. In the region of 265–325 nm of the CD spectra, it belonged to the chiral BINOL unit exhibiting two characteristic CD signals at about 265 and 288 nm [31]. However, in the longer wavelength region, one strong signal at *ca.* 341 nm with a crossover point at 386 nm, one weaker signal at *ca.* 400 nm as well as a moderate signal at *ca.* 550 nm, are mainly attributed to the helical π-system of naphthalene annulated **PDIs**. Accordingly, the incorporation of chiral BINOL units into the **PDIs** indeed leads to the chiral transfer from BINOL to BPDH molecules. Similar conclusions can also be drawn from the fluorescence spectra of **R/S-BPDH** that exhibit obvious mirror-image CPL signals with the emission maxima at around 600 nm (Fig. 4).

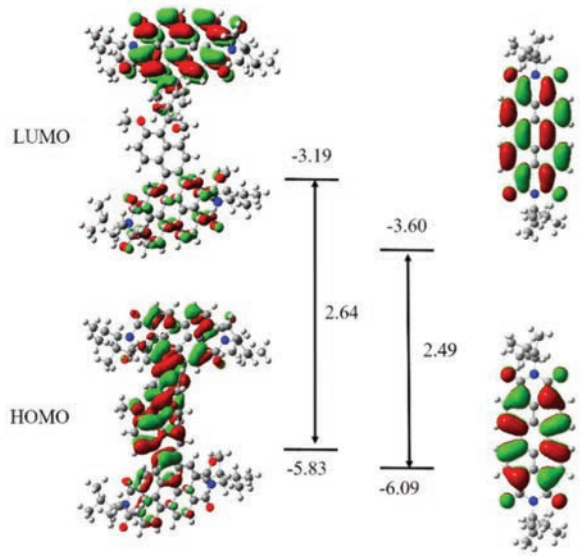

Fig. 3. The frontier orbitals of **R/S-BPDH** and **PDIs** corresponding energy levels and energy gap calculated in Gaussian 09 at the B3LYP/6–31G(d, p) level by DFT. The structures of **R/S-BPDH** are optimized from conformational searching (unit: eV).

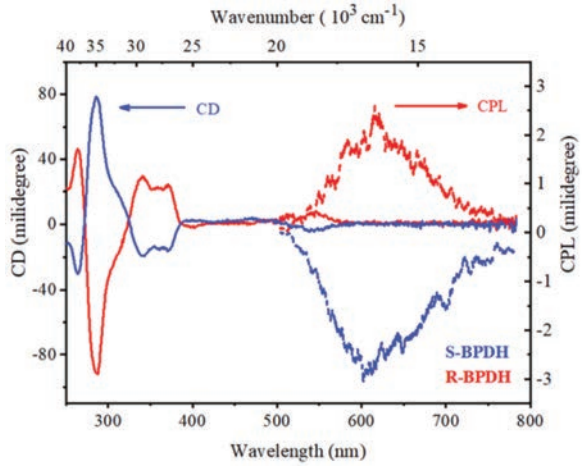

Fig. 4. The CD and CPL spectra of **R/S-BPDH** in DCM (5×10^{-6} mol/L, $\lambda_{ex} = 470$ nm) at the room temperature.

As stated above, due to the rotatable C–C bonds in **R/S-BPDH**, the fluorescence intensities are quenching in the solvents, but possibly enhanced in the aggregates. To validate this speculation, their UV–vis absorption and fluorescence properties have been investigated in mixture solvents (5×10^{-6} mol/L) of good solvent DCM and poor solvent MCH with different ratios. In the mixture solvents of DCM/MCH, with the increasing the MCH ratio from 0% to 90%, their absorption maxima are blue-shifted slightly. Meanwhile, their spectral shapes become sharper and sharper with the gradual appearance of their shoulder-bands at the longer wavelength and the intensity at the absorption maxima decrease gradually from 124,260 L mol^{-1} cm^{-1} to 102,988 L mol^{-1} cm^{-1} (Fig. S22 in Supporting information). These spectral changes might be attributed to two factors: one is the reduced ICT transitions in polar DCM solvent with the increasing ratio of nonpolar MCH, and another is the improved molecular rigidity upon the aggregations, which could be magnified in their fluorescence spectra. As shown in Fig. 5 and Fig. S23 (Supporting information), with the increasing ratio of MCH from 0% to 90%, their emission maxima are blue-shifted remarkably from 601 nm to 562 nm, accompanied by the quantum yield

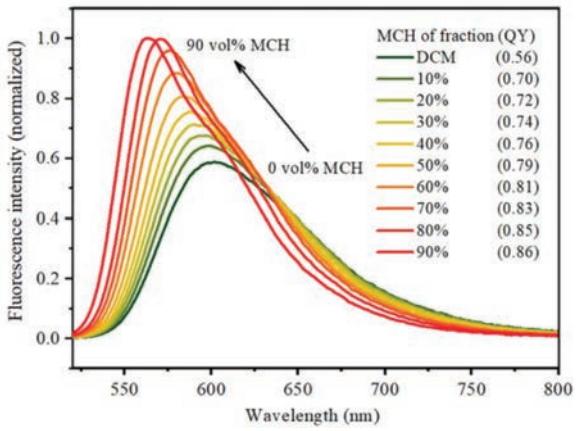

Fig. 5. The fluorescence spectrum of **R-BPDH** in a mixture solvent of DCM and MCH with different ratios in a fixed concentration (5×10^{-6} mol/L).

increased gradually from 0.56 to 0.86. Accordingly, the blue-shifted emissions might be governed by the reduced ICT transitions, while the enhanced emissions are more likely by the improved rigidity, particularly the rotation restrictions of **R/S-BPDH** in the aggregated states.

Similarly, the CD and CPL properties of **R/S-BPDH** have also been studied in mixture solvents of DCM/MCH (5×10^{-6} mol/L) with different ratio (Figs. S24 and S25 in Supporting information). As shown in Fig. 6a, in a mixture solvent of DCM/MCH (1:9 in volume), the characteristic CD signals assigned to the BINOL units at *ca.* 288 nm became fewer for both **R/S-BPDH** in comparison to those in pure DCM. More interestingly, their CD signals are totally reversed in the region of 340–400 nm, accompanied by the significantly enhanced signals between 480 and 550 nm in the opposite direction. Obviously, the weakened signals at *ca.* 288 nm are attributed to the possibly smaller dihedral angles of **R/S-BPDH** in the aggregated states compared to those in the DCM [32], while the reversed signals, particularly those enhanced reversed signals are related to the generation of chiral aggregates with the opposite chirality to those of their monomers, respectively. Similar conclusions on the aggregation-induced chirality inversion can also be drawn from their CPL studies, which exhibit the reversed CPL signals upon addition 90% MCH into DCM (Fig. 6b). Notably, the CPL intensities are much more enhanced, which is consistent with the enhanced reversed signal in their CD spectra.

To further explore the aggregated structures of **R/S-BPDH**, we have attempted to obtain their self-assembled samples from the DCM/MCH (1:9 in volume) solutions. Fortunately, a small amount of precipitation was collected for **R-BPDH** when the concentration increased to 5.6×10^{-5} mol/L upon standing for several days. The transmission electron microscopic studies reveal that the precipitation is 1-D fibers (Fig. S26 in Supporting information). Due to the low resolutions, no chiral morphologies have been detected. In addition, the powder X-ray diffraction (PXRD) measurement of this precipitation indicate in the wide angle region, an obvious diffraction peak with a *d*-spacing of 3.16 Å was observed (Fig. S27 in Supporting information), demonstrating that there is strong π-π stacking in the aggregated **R-BPDH** [33]. More importantly, the temperature-dependent UV–vis absorption spectral investigations of **R/S-BPDH** in pure MCH show that the spectral shapes are similar to those in pure DCM at high temperature (80 °C). However, the remarkable feature is the gradual appearance of a new absorption band at the long wavelength side when cooling to low temperature (25 °C). Together with the bulk substituent at the imide position, the new absorption band should be attributed to the cross stacking between two naphthalene annulated PDI unit from neighbor-

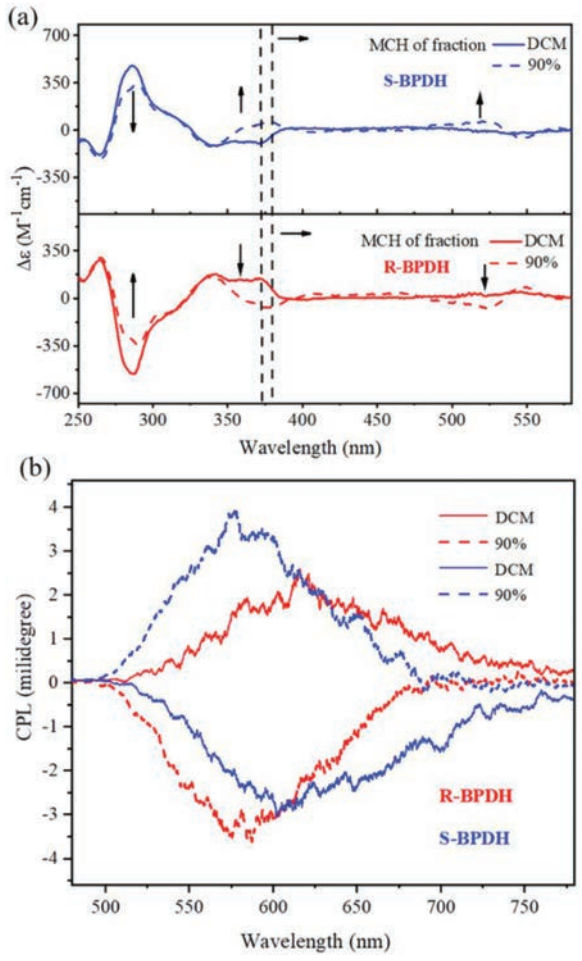

Fig. 6. The CD (a) and CPL (b) spectra of **R/S-BPDH** in pure DCM and a mixture solvent of DCM and MCH with a volume ratio of 1:9 (5×10^{-6} mol/L).

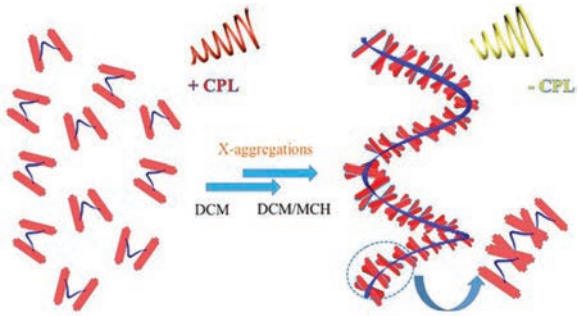

Fig. 7. Schematic representation of the possible packing for **R-BPDH** in aggregated states.

ing two **R-** or **S-BPDH** molecules (Fig. S28 in Supporting information). This deduction is indeed be substantiated by concentration-dependent ^{1}H NMR spectroscopy (Fig. S29 in Supporting information), which exhibits that two singlet peaks in the lower field (10.0–10.6 ppm) assigned to the *para*-H close to imide positions are gradually shifted to the higher field due to the shielding effect. Therefore, a plausible molecular packing for **R-BPDH** in the aggregated state could be proposed. As shown in Fig. 7, due to the bulk substituent at the imide position, the neighboring two PDI units from two **R-BPDH** molecules are inclined to adopt a cross-stacking mode. Besides, because of the steric hindrance of the imide substituent in the chiral BINOL corer (helical π-clips), two **R-BPDH** molecules are stacking against each other and thus forming a 1-D helical structure with opposite chirality (M).

In summary, we reported a pair of novel enantiomerically pure **PDIs** derivatives, **R/S-BPDH** by the annulation of *R*/*S*-1,1′-binaphthol into perylene diimide dyes at the bay position. To the best of our knowledge, such axially chiral perylene dyes with red CPL emission is unprecedented. More importantly, the spectral studies reveal that two unusual phenomena, AIEE and aggregation-induced chirality inversion, were observed simultaneously for the first time. Thus, further studies on this unique class of chiral **PDIs** derivatives in various directions are well motivated.

Declaration of competing interest

The authors declare that they have no known competing financial interests or personal relationships that could have appeared to influence the work reported in this paper.

Acknowledgments

This work is financially supported by the National Natural Science Foundation of China (No. 21971041) and Natural Science Foundation of Fujian Province (No. 2020J01447).

Supplementary materials

Supplementary material associated with this article can be found, in the online version, at doi:10.1016/j.cclet.2021.11.069.

References

[1] F. Saal, F.Y. Zhang, M. Holzapfel, et al., J. Am. Chem. Soc. 142 (2020) 21298–21303.
[2] G.P. Gao, N.N. Liang, H. Geng, et al., J. Am. Chem. Soc. 139 (2017) 15914–15920.
[3] S.W. Thomas III, G.D. Joly, T.M. Swager, Chem. Rev. 107 (2007) 1339–1386.
[4] J.D. Luo, Z.L. Xie, J.W.Y. Lam, et al., Chem. Commun. (2001) 1740–1741.
[5] B.K. An, S.K. Kwon, S.D. Jung, S.Y. Park, J. Am. Chem. Soc. 124 (2002) 14410–14415.
[6] M.T. Chen, Y. Zhang, M.O. Vysotsky, et al., Org. Chem. Front. 6 (2019) 3731–3740.
[7] Y.Y. Li, S.J. Liu, H.W. Ni, et al., Angew. Chem. Int. Ed. 59 (2020) 12822–12826.
[8] F. Würthner, Angew. Chem. Int. Ed. 59 (2020) 14192–14196.
[9] L.W. Ma, C.P. Li, Q. Yan, et al., Chin. Chem. Lett. 31 (2020) 361–364.
[10] Y.J. Kong, Z.P. Yan, S. Li, et al., Angew. Chem. Int. Ed. 59 (2020) 5336–5340.
[11] J.J. Guo, J.Z. Fan, X.Z. Liu, et al., Angew. Chem. Int. Ed. 59 (2020) 8828–8832.
[12] V. Krishnasamy, W. Qu, C.L. Chen, et al., Macromolecules 53 (2020) 4193–4203.
[13] S. Ogi, V. Stepanenko, K. Sugiyasu, et al., J. Am. Chem. Soc. 137 (2015) 3300–3307.
[14] K. Takaishi, K. Iwachido, T. Ema, J. Am. Chem. Soc. 142 (2020) 1774–1779.
[15] Y. Sheng, D. Shen, W.J. Zhang, et al., Eur. J. Chem. 21 (2015) 13196–13200.
[16] Q. Ye, F. Zheng, E.Q. Zhang, et al., Chem. Sci. 11 (2020) 9989–9993.
[17] W. Jiang, Y. Li, Z.H. Wang, Acc. Chem. Res. 47 (2014) 3135–3147.
[18] M.J. Lin, B. Fimmel, K. Radacki, F. Würthner, Angew. Chem. Int. Ed. 50 (2011) 10847–10850.
[19] Z.T. Liu, Y. Wu, Q. Zhang, X. Gao, J. Mater. Chem. A 4 (2016) 17604–17622.
[20] Z.T. Liu, L.H. Zhang, M. Shao, et al., ACS. Appl. Mater. Interfaces 10 (2018) 762–768.
[21] H.T. Feng, X.G. Gu, J.W.Y. Lam, Y.S. Zheng, B.Z. Tang, J. Mater. Chem. C 6 (2018) 8934–8940.
[22] E.M. Sanchez-Carnerero, F. Moreno, B.L. Maroto, et al., J. Am. Chem. Soc. 136 (2014) 3346–3349.
[23] F.Y. Song, Z. Zhao, Z.Y. Liu, J.W.Y. Lam, B.Z. Tang, J. Mater. Chem. C 8 (2020) 3284–3301.
[24] D.H. Lim, Y.J. Kim, Y.A. Kim, et al., Chem. Mater. 31 (2019) 4629–4638.
[25] B. Liu, M. Bockmann, W. Jiang, N.L. Doltsinis, Z.H. Wang, J. Am. Chem. Soc. 142 (2020) 7092–7099.
[26] R. Mishra, J.M. Lim, M. Son, et al., Eur. J. Chem. 20 (2014) 5776–5786.
[27] L.H. Feng, Y. Wang, F. Liang, M. Xu, X.J. Wang, Tetrahedron 67 (2011) 3175–3180.
[28] H. Langhals, O. Krotz, K. Polborn, P. Mayer, Angew. Chem. Int. Ed. 44 (2005) 2427–2428.
[29] L. Li, Y.J. Hong, D.Y. Chen, M.J. Lin, Eur. J. Chem. 23 (2017) 16612–16620.
[30] Q. Zhang, S.R. Cohen, I. Rosenhek-Goldian, et al., J. Phys. Chem. C 123 (2019) 25031–25041.
[31] L.Di Bari, G. Pescitelli, P. Salvadori, J. Am. Chem. Soc. 121 (1999) 7998–8004.
[32] H.K. Zhang, H.K. Li, J. Wang, et al., J. Mater. Chem. C 3 (2015) 5162–5166.
[33] P. Rajamalli, E. Prasad, Org. Lett. 13 (2011) 3714–3717.